Runoff-driven export of particulate organic carbon from soil in temperate forested uplands

Joanne C. Smith[1], Albert Galy[1], Niels Hovius[1,2], Andrew M. Tye[3], Jens M. Turowski[4], Patrick Schleppi[4]

[1]Department of Earth Sciences, University of Cambridge, Cambridge, UK

[2]Present address: German Research Centre for Geosciences GFZ, Potsdam, Germany

[3]British Geological Survey, Keyworth, Nottingham, UK

[4]Swiss Federal Research Institute WSL, Birmensdorf, Switzerland

Corresponding author:
J. C. Smith
Department of Earth Sciences, University of Cambridge, Downing Street, Cambridge CB2 3EQ, UK
jcs74@cam.ac.uk
Phone: +44 (0)1223 333455
Fax (department reception): +44 (0)1223 333450

Abstract

We characterise the sources, pathways and export fluxes of particulate organic carbon (POC) in a headwater catchment in the Swiss Alps, where suspended sediment has a mean organic carbon concentration of 1.45% ± 0.06 . By chemically fingerprinting this carbon and its potential sources using carbon and nitrogen elemental and isotopic compositions, we show that it derives from binary mixing between bedrock and modern biomass with a soil-like composition. The hillslope and channel are strongly coupled, allowing runoff to deliver recent organic carbon directly to the stream beyond a moderate discharge threshold. At higher flows, more biomass is mobilized and the fraction of modern carbon in the suspended load reaches 0.70, increased from 0.30 during background conditions. Significant amounts of non-fossil organic carbon are thus transferred from the hillslope without the need for extreme events such as landsliding. Precipitation is key: as soon as the rain stops, biomass supply ceases and fossil carbon again dominates. We use rating curves modeled using samples from five storm events integrated over 29-year discharge records to calculate long-term export fluxes of total POC and non-fossil POC from the catchment of 23.3 ± 5.8 and 14.0 ± 4.4 tonnes km^{-2} yr^{-1} respectively. These yields are comparable to those from active mountain belts, yet the processes responsible are much more widely applicable. Such settings have the potential to play a significant role in the global drawdown of carbon dioxide via riverine biomass erosion, and their contribution to the global flux of POC to the ocean may be more important than previously thought.

Keywords

Organic carbon, stable isotope geochemistry, carbon export, mountain rivers, runoff processes

1. Introduction[1]

Export and deep marine burial of carbon from plants and soils, recently fixed from the atmosphere by photosynthesis, transfers carbon from the atmosphere into geological storage (e.g. Berner, 1982; France-Lanord and Derry, 1997). Previous work on carbon export from catchments has focused on active mountain belts because of their importance in the physical erosion budget (Milliman and Syvitski, 1992). For example, recent studies (Carey et al., 2005; Hilton et al., 2008a, 2008b; Lyons et al., 2002) suggest that storm-driven erosion of terrestrial biomass can effectively sequester carbon in tectonically and climatically extreme regimes, such as the active mountain belts of Taiwan and New Zealand. Deep-seated landslides and gully erosion are important in mobilising particulate organic carbon (POC) in extreme events in these environments (Hilton et al., 2008a; West et al., 2011). This POC consists of both modern POC from biomass and fossil POC from sedimentary bedrock. However, there are also indications that erosion processes associated with less intense runoff, driven directly by precipitation, may also be important, particularly in shifting the balance of POC carried in the suspended load towards non-fossil sources (Gomez et al., 2010; Hilton et al., 2012a, 2008b). While deep landslides and gully erosion mobilize bedrock as well as POC, runoff erosion via

[1] Abbreviations used throughout the article:
POC: particulate organic carbon
tPOC: total particulate organic carbon
fPOC: fossil particulate organic carbon
nfPOC: non-fossil particulate organic carbon
C_{org}: organic carbon concentration
SS: suspended sediment
SSC: suspended sediment concentration
TSL: total suspended load
F_{nf}: modeled fraction of non-fossil organic carbon
F_{mod}: fraction of non-fossil organic carbon obtained from radiocarbon measurements
Q_e: effective discharge

overland flow removes only the surface layer of soil (Horton, 1945). If such processes are significant, the harvest of non-fossil POC stored in plants and soils could happen anywhere that there is enough rain on vegetated hillslopes to generate overland flow or shallow landslides.

Evidence for terrestrial POC export in temperate settings unaffected by rapid uplift and tropical storms exists in marine sediments (Gordon and Goñi, 2003; Prahl et al., 1994) and in inputs to the ocean (Hatten et al., 2012), but there is still insufficient understanding of the processes which mobilize POC in the headwater source areas of these deposits. Here, we investigate POC sources and initial pathways under changing hydrologic conditions in a temperate, partly forested headwater catchment in the Swiss Prealps, where the runoff effect is not normally masked by deep-seated landsliding. We find strong evidence for runoff-driven transfer of significant amounts of modern soil-derived biomass during moderate hydrologic conditions, with the proportion of modern carbon in the suspended load increasing with discharge.

2. Study Site

The Erlenbach is a first order tributary of the Alp River, located 40 km south of Zurich near the town of Einsiedeln. It has a small catchment area (0.74 km^3), elevation 1110 to 1655 m above sea level and average slope of 20% (Hagedorn et al., 2000). The mean annual air temperature is 6 °C and mean annual precipitation is 2300 mm (Hagedorn et al., 2001), 800 mm of this falling as snow in winter (Schleppi et al., 2005). The largest precipitation events occur as convective rainfall during the summer. In common with other small mountain river systems (Wheatcroft et al., 2010), discharge rises quickly during storms and is highly episodic in response to rainfall (Schleppi et al., 2006).

The catchment is developed on pelitic turbidites of the Eocene Wägital-Flysch Formation (Winkler et al., 1985). Recent glacial till overlies these rocks, particularly at lower elevations with a cover of up to several metres thick on the lower left bank. Both bedrock and drift are fine-grained, clay-rich and impermeable, resulting in water-saturated gleysols. Creep landslides are common, particularly in the lower reaches where steep channel sides cut into active complexes developed mainly in the till. These incrementally deliver substantial amounts of sediment to the stream channel during winter, which is removed by summer storms (Schuerch et al., 2006). The Erlenbach lacks a well-developed riparian zone and has a step-pool morphology with both logs and boulders forming the steps (Turowski et al., 2009). The catchment is 40% forest and 60% wetland and alpine meadow (Turowski et al., 2009). The main tree species are Norway Spruce (*Picea abies*) and European Silver Fir (*Abies alba*), with some green Alder (*Alnus viridis*) (Schleppi et al., 1999).

The Erlenbach is an experimental catchment of the Swiss Federal Institute for Forest, Snow and Landscape Research (WSL) (Hegg et al., 2006). Over the time period 1983-2011 inclusive, discharge (Q) recorded at 10-minute intervals ranged from 0 to 11946 l s^{-1} with an average (Q_{mean}) of 38.6 l s^{-1}. In this study, we report discharges relative to this value (as Q/Q_{mean}), as well as absolute values, to allow comparison to other catchments. Over the monitoring period, flow was less than or equal to Q_{mean} for 77% of the time, with such discharges accounting for about 1% of suspended sediment transport. Less than 1% of discharges were above the threshold at which substantial bedload transport starts, which corresponds to Q/Q_{mean} ~13 (Turowski et al., 2011). The catchment is also a site for the NITREX project (NITRogen saturation EXperiments) (Wright and Rasmussen, 1998), and has three <1 ha sub-plots equipped with V-notch weirs in forest, forest with experimental nitrogen addition, and meadow (Schleppi et al., 1998).

3. Methods

POC in riverine suspended sediment is a mixture of carbon from two or more end member sources (Blair et al., 2003; Hilton et al., 2008a, 2008b; Komada et al., 2004; Leithold et al., 2006). It is particularly important to distinguish between carbon from fossil and non-fossil sources, because re-burial of fossil carbon has no effect on contemporary CO_2 drawdown, while burial of non-fossil carbon bypasses the usual rapid oxidation pathway and sequesters carbon (Berner, 1982). Mixing relationships can be primarily elucidated in N/C-δ^{13}C and C/N-δ^{15}N space (e.g. Hilton et al., 2010), while ^{14}C provides an additional constraint on the input of fossil carbon (e.g. Blair et al., 2003; Hilton et al., 2008b; Komada et al., 2005).

3.1 Sample Collection

Instantaneous suspended sediment samples were collected direct from the stream at the upper gauging station in 100 ml plastic bottles, every few minutes during five storm events in July 2010. The largest of these (12 July) had a return period of about one year and a peak discharge of 2290 l s^{-1}, corresponding to a Q/Q_{mean} of ~59. The remaining four events took place within 10 days and covered a range of peak discharges from 300 to 1580 l s^{-1} [Table 1]. With the exception of the 12 July event, the storms were characterised by intermittent rain. The hydrographs for three of the events are shown in Figure 1. After collection, each turbid sample was passed through a 0.2 μm nylon filter within two weeks (mostly within three days), following interim storage at 5 °C. The filters with sediment were stored in glass petri dishes at -18 °C before lyophilization.

110 samples from potential sources for the riverine suspended sediment, including bedrock, surface soil, deeper soil profiles, foliage, wood, bedload and material from landslides and banks adjoining the channel, were collected between October 2009 and August 2010. All samples were stored in sealed plastic bags and oven-dried in covered foil dishes at <80 °C as soon as possible (1-12 days) after collection.

Surface soil and foliage were collected in transects across the catchment at a range of elevations, covering all major geomorphologic and ecologic conditions. At each locality, samples as representative as possible of the immediate surroundings were taken. Surface soil (a combination of O and A layers) was collected from the top ~10 cm with a clean trowel, after removal of overlying vegetation. Although the timing of collection could potentially affect the isotopic composition of soil samples because more decomposed litter could be enriched in ^{13}C and ^{15}N (e.g. Dijkstra et al., 2008), the collection method and subsequent processing result in samples homogenised over a long enough period to negate any seasonal differences. Foliage included multiple samples, comprising needles, leaves and twigs from all sides, of the three main tree types and representative understory. Samples of woody debris embedded in landslides and the channel bed were also collected across the catchment. Throughout this study, ‘foliage’ and ‘wood’ are used as convenient terms for different types of standing biomass, and include all associated microbial organisms.

Two vertical profiles were taken through landslides (down to 80 cm and 170 cm), and two through stable hillslopes (to 60 cm and 160 cm); these were sampled at 10-60 cm intervals. In reporting the results, the uppermost soil samples from each stable hillslope profile are treated as ‘surface soils’ and are excluded from the profile group (‘deep soils’). Soil is generally poorly developed on top of the landslides and so no such distinction is made. 22 bedrock samples were obtained across the catchment (from both hillslopes and stream bed). Bedload was collected along the full length of the main channel.

Discharge-proportional compound samples of suspended sediment were collected from the forest control and meadow sub-plots weekly (when there was enough runoff) between August 2009 and August 2011. A representative subset of each of these was analyzed to obtain an estimate of the hillslope input signal.

3.2 Sample Preparation

For source sediments, only the suspendable fraction (<2 mm), isolated through wet- and dry-sieving, was subjected to further analysis. Suspended sediment occasionally contained material >2 mm; these particles, mainly large organic material such as spruce or fir needles, were excluded from chemical analysis, though their weight was recorded and used in calculations of suspended sediment concentrations. Bedrock and vegetation samples were analyzed in bulk.

All samples were homogenized using either a ball mill grinder, a pestle and mortar (for small samples) or a blade mill grinder (for vegetation). Bedrock samples were first crushed using a jaw crusher to fragments <5 mm. Pulverized samples and blanks were heated to 80 °C with dilute (1M) hydrochloric acid for three hours to remove carbonate, rinsed with de-ionized water and dried thoroughly (France-Lanord and Derry, 1994; Galy et al., 2007a; Hilton et al., 2008a). Between 5 and 30% of each sample was lost through the carbonate removal process, with no apparent disparity between different types of material. Most of this loss corresponds to carbonate dissolution plus loss of particles on the vessels used in treatment (Galy et al., 2007a; Hilton et al., 2008a; Brodie et al., 2011). This process unavoidably causes loss of a labile fraction of organic C, and the results reported here relate to the non-labile fraction only. However, it is this more recalcitrant fraction that is most likely to be ultimately buried in the ocean, and therefore of interest in this study. This procedure was carried out on all samples (including vegetation), so that any isotopic fractionation effects of the de-carbonation process (Brodie et al., 2011) are universally applied and the results are internally consistent.

3.3 Analysis

Processed, powdered samples were combusted, and the resultant N_2 and CO_2 concentrations (reported in weight %) and carbon and nitrogen isotopic compositions ($\delta^{13}C$ and $\delta^{15}N$, reported in ‰) were obtained using a flash Elemental Analyser coupled to a continuous flow Nier-type mass spectrometer via a gas bench for gas separation. All measurements were corrected for procedural blanks following published methods (Hilton et al., 2010; 2012b). Multiple aliquots of varying material were analyzed; the average relative difference was <<0.001% for C and N, and average standard deviation was 0.05‰ for $\delta^{13}C$ and 0.3‰ for $\delta^{15}N$. To test for long-term machine drift, 10 samples were analyzed a second time one year after the first analysis. This set of repeats had an average relative difference of 0.06% for C and 0.07% for N, and average standard deviation of 0.05‰ for $\delta^{13}C$ and 0.3‰ for $\delta^{15}N$.

^{14}C measurements on 14 graphitized samples were obtained by accelerator mass spectrometry at the NERC Radiocarbon Laboratory in East Kilbride, UK. Reported results comprise the proportion of ^{14}C atoms in each sample compared to that present in the year 1950 (F_{mod}), $\Delta^{14}C$ in ‰, and conventional radiocarbon age. The standard IAEA-C5, subjected to the same carbonate-removal procedure as the samples, returned ^{14}C to within 1σ of the consensus value.

4. Results

4.1 Concentration and Composition of Organic Carbon in Source Materials

Composition data for riverine suspended sediment, hillslope runoff input and major carbon stores within the catchment are summarised in Table 2 while the radiocarbon data are shown separately in Table 3.

Bedrock has organic carbon concentrations (C_{org}) ranging from 0.16-1.15%, with a mean of 0.54% ± 0.11 (± $2\sigma_{mean}$, n = 22), C/N of 7.81 ± 1.7, $\delta^{13}C$ =-25.71‰ ± 0.36 and $\delta^{15}N$ =3.34‰ ± 0.26. Bedload, channel banks and landslide deposits have similarly low C_{org} (all means <1%), and are compositionally very similar to bedrock. Modern sources, surface soil (n = 17) and foliage (n = 8), have significantly higher C_{org} (16.5% ± 6.3 and 46.9% ± 2.0 respectively). Both pools have high C/N and are depleted in heavy isotopes of C and N, but do not overlap: surface soil has C/N of 17.9 ± 2.2, $\delta^{13}C$ of -26.84‰ ± 0.48 and $\delta^{15}N$ of -1.33‰ ± 0.76, while foliage has C/N of 55.5 ± 17, $\delta^{13}C$ of -28.30‰ ± 1.13 and $\delta^{15}N$ of -5.87‰ ± 1.67. The ^{14}C results from surface soils show that they are essentially modern; the one soil F_{mod} value of less than 1 is explained by its close association with a landslide and lack of overhead forest canopy. Woody debris (up to 4000 years old) have high C_{org} (49.1% ± 1.8; n = 12), high C/N (173 ± 98), are depleted in ^{15}N ($\delta^{15}N$ =-3.99‰ ± 1.29), and enriched in ^{13}C ($\delta^{13}C$ =-25.25‰ ± 0.69), in contrast to modern vegetation.

Landslide complexes have homogeneous compositions throughout their depth, with no systematic variations in C_{org}, C/N, $\delta^{13}C$ or $\delta^{15}N$. In contrast, the soil profiles from stable slopes show a significant decrease in C_{org} and C/N (to levels comparable to the landslides) at ~40-60 cm depth, although there are no clear patterns in isotopic composition. The landslide profiles sampled show very little incorporation of non-fossil material, while the soil profiles (even without the uppermost samples) document a transition from surface-like horizons to a more fossil-like layer at depth.

4.2 Concentration of Organic Carbon in Riverine Suspended Sediment

The observed range of C_{org} in riverine suspended sediment samples was 0.78-2.52%, with a mean of 1.45% ± 0.06 (±2σ_{mean}, n = 122). Within each event, there appears to be no consistent pattern in C_{org} over the hydrograph [Figure 1]. However, when all data are considered together, there is a clear parabolic pattern in the variation of C_{org} with both Q and suspended sediment concentration (SSC), with negligible difference in C_{org} patterns between rising and falling limbs. The product of Q and SSC combines both effects in the parameter 'total suspended load' (TSL, in g s^{-1}) [Figure 2]. At low TSL, C_{org} is initially variable, then decreases with increasing TSL. Beyond a threshold of ~500 g s^{-1} (corresponding to Q/Q_{mean} ~10 and SSC ~1600 mg l^{-1}), C_{org} increases: this trend continues up to at least ~40000 g s^{-1} (Q/Q_{mean} ~60). The threshold is reached under moderate conditions, occurring several times per year, and in four of the five events sampled. Because of this change in behaviour, we take flows of Q/Q_{mean} <10 to represent background conditions, after Gomez et al. (2010).

4.3 Composition of Organic Carbon in River and Runoff Suspended Sediment

C/N ranges from 6.9 to 13, with a mean of 9.55 ± 0.24 ($\pm 2\sigma_{mean}$, n = 122); $\delta^{13}C$ ranges from -27.55 to -24.25‰ with a mean of -26.33‰ ± 0.08; and $\delta^{15}N$ ranges from 0.15 to 5.08‰ with a mean of 2.21‰ ± 0.16. There are compositional differences between samples collected on the rising and falling limbs, and during rain and dry periods [Table 2], with the former group having higher C/N and lower $\delta^{13}C$ and $\delta^{15}N$ in each case. The mean F_{mod} for the six suspended sediment samples sent for $\Delta^{14}C$ analysis was 0.65 ± 0.08 ($\pm 2\sigma_{mean}$, n = 6). In both N/C-$\delta^{13}C$ and C/N-$\delta^{15}N$ compositional space where mixing relationships are linear, POC in riverine suspended sediment samples plots in a broadly linear range bounded approximately by bedrock and soil [Figure 3]. Suspended sediment samples with higher $\delta^{15}N$ than the bedrock range may indicate that the stream is sampling bedrock compositions not exposed at the surface elsewhere in the catchment.

In contrast to most pools, the mean composition of carbon in the hillslope runoff suspended sediment samples suggests different relationships in the N/C-$\delta^{13}C$ and C/N-$\delta^{15}N$ plots. In N/C-$\delta^{13}C$ space, forest and meadow runoff samples have the same composition within error, and lie at the low-N/C, low-$\delta^{13}C$ end of the riverine suspended sediment range. In C/N-$\delta^{15}N$ space, forest and meadow runoff are compositionally distinct, and both lie outside the compositional range of riverine suspended sediment [Figure 3]. Both sets of runoff samples have higher C_{org} values than riverine suspended sediment, of 9.12% ± 0.9 ($\pm 2\sigma_{mean}$, n = 38; forest) and 15.9% ± 1.7 ($\pm 2\sigma_{mean}$, n= 10; meadow).

5. Discussion

Both the compositional distribution and F_{mod} values of riverine suspended sediment are consistent with mixing between fossil and non-fossil end members. Although C_{org} in the suspended sediment is always higher than that of bedrock, indicating that there is some non-fossil input at all times, this input becomes increasingly significant at higher TSL and Q [Figure 4]. POC from samples collected at low TSL cover the whole compositional range, but are strongly concentrated towards low C/N and high $\delta^{13}C$ and $\delta^{15}N$ (that is, a 'fossil' composition). During larger events, there is a bulk shift away from the fossil towards the non-fossil end of the mixing line.

5.1 Nature of the Non-Fossil End Member

Because the composition of the POC exported from the catchment plots in the space between several different carbon pools, careful definition of the end members is necessary. Although the ‘fossil’ chemical composition of bedload, landslides and channel banks suggests that these pools all derive from bedrock, we take bedrock alone as the unequivocal fossil end member. Of the non-fossil carbon pools, surface soil and foliage are closest to but not exactly on the mixing trend defined by bedrock and the suspended sediment samples. Non-fossil material comes from a range of sources, so we calculate a hypothetical non-fossil end member using F_{mod} and $\delta^{13}C$ following the procedure defined by Hilton et al. (2010). Briefly, the $\delta^{13}C$ of the individual non-fossil end member for each suspended sediment sample with known F_{mod} is calculated according to the mixing relationship

$$\delta^{13}C_{sample} = F_{mod}.\delta^{13}C_{nf} + (1-F_{mod}).\delta^{13}C_{fos}$$

where $\delta^{13}C_{nf}$ and $\delta^{13}C_{fos}$ are the $\delta^{13}C$ values of a hypothetical non-fossil end member and the average $\delta^{13}C$ of bedrock samples respectively. The mean of the six calculated values of $\delta^{13}C_{nf}$ is taken. We then use lines of best fit, calculated using only points with $Q/Q_{mean} > 10$, to find the corresponding N/C, C/N and $\delta^{15}N$. Uncertainties of twice the standard error on the mean of the initial $\delta^{13}C$ value are propagated through this calculation procedure. The resulting hypothetical end member [Figure 4] has C/N of 15.8 ± 6.8, $\delta^{13}C$ of -27.15‰ ± 0.53 and $\delta^{15}N$ of 0.61‰ ± 1.40. This is much more similar to surface soil than foliage, suggesting that soil is heavily implicated in the non-fossil POC input. It is also similar to the forest hillslope runoff signal in N/C-$\delta^{13}C$ space, but the two have distinctly different $\delta^{15}N$ values.

The concentrations of fossil and non-fossil POC in milligrams per litre can be obtained for each sample, and then used to determine independent relationships with discharge, if we know the proportion of organic carbon derived from non-fossil sources. Given the simple mixing exhibited by the system, it is possible to model this parameter for each suspended sediment sample, denoted F_{nf} to distinguish it from F_{mod} measured using ^{14}C, using the mixing equation given above, the $\delta^{13}C$ of the sample and two end members (Hilton et al., 2010). We used bedrock and the hypothetical non-fossil end member determined above. Owing to scatter in the system, calculated F_{nf} values for 9% of the samples fell outside the possible range of 0-1.1. For these, a value of 0 or 1.1 was substituted as appropriate. On the samples sent for ^{14}C analysis, F_{nf} shows reasonable agreement with F_{mod}, reproducing it to within 0.24 at the 95% level.

5.2 Long-Term Carbon Export Flux: Fossil and Non-Fossil Components

It is important to consider not only the export of total carbon, but of fossil carbon and non-fossil carbon separately, because only non-fossil carbon burial has an effect on contemporary carbon dioxide drawdown (e.g. Berner, 1982; Blair and Aller, 2012). Because distinct pools of organic carbon behave differently, shown by the changing composition of POC at different discharges, their long-term export should be considered independently (Wheatcroft et al., 2010).

We used the calculated F_{nf} values to construct rating curves describing the relationships between discharge and load of four components: suspended sediment (SS), total POC (tPOC), fossil POC (fPOC) and non-fossil POC (nfPOC). These are all power laws of the form $a(Q/Q_{mean})^{b}$ [Table 4; Figure 5]. Because of the threshold switch to POC addition at $Q/Q_{mean} > 10$, and the fact that flows above background conditions are disproportionately important in transporting sediment and POC, we would ideally only use samples at Q/Q_{mean} >10 to fit the rating curves. However, this is mathematically unsatisfactory as it restricts the range of Q/Q_{mean} to less than one order of magnitude and results in large uncertainties on *a* and *b*. We therefore use relationships determined using the full sample set (three orders of magnitude in Q/Q_{mean}), but check their geomorphological validity by comparing with those determined using only samples with Q/Q_{mean} >10, finding in all cases that *a* and *b* are well within error [Table 4].

The larger exponent for tPOC (*b* = 1.33) compared to SS (*b* = 1.19) means that relatively more POC is exported at higher discharges than SS, in contrast to the relationships seen in the Waipaoa River (New Zealand) and Alsea River (Oregon) (Wheatcroft et al., 2010). The effect is even more pronounced for nfPOC (*b* = 1.45) than for tPOC. The exponent for fPOC (*b* = 1.08) is within error of that for SS, reflecting their shared clastic origin. Differences in the rating curve exponents are mirrored by those in effective discharge (Q_e), the discharge that, on average, transports the largest proportion of a given constituent load (Andrews, 1980; Nash, 1994; Wheatcroft et al., 2010). Q_e is greatest for nfPOC (corresponding to Q/Q_{mean} of 13.4), and lowest for fPOC (5.6). Q_e for all four components [Table 4] corresponds to similar flows (relative to Q_{mean}) to many other small mountain rivers (Wheatcroft et al., 2010).

Applying these rating relationships to the discharge record for the Erlenbach, we modeled the export of the four components over the period 1983-2011 inclusive, with full results shown in [Table 5]. The mean annual yields and export fluxes of each component were: 1220 ± 232 t yr^{-1} and 1648 ± 313 t km^{-2} yr^{-1} (SS); 17.3 ± 4.3 t yr^{-1} and 23.3 ± 5.8 t km^{-2} yr^{-1} (tPOC); 7.4 ± 1.2 t yr^{-1} and 10.1 ± 1.6 t km^{-2} yr^{-1} (fPOC); and 10.4 ± 3.2 t yr^{-1} and 14.0 ± 4.4 t km^{-2} yr^{-1} (nfPOC). These amounts of fossil and non-fossil carbon exported were used to calculate a mean F_{nf} value for each year, both overall and at different discharges [Table 5]. According to the model, 61% of all the organic carbon exported from the Erlenbach over this 29-year period came from non-fossil sources (mean overall F_{nf} = 0.61 ± 0.02).

The yield of fPOC based on rating curve [Table 5] is within error of the 'expected' mean annual yield of fossil carbon (7.3 ± 1.3 t yr^{-1}), reached by multiplying the average C_{org} of the bedrock samples by suspended sediment yield. This suggests that there is no significant remineralization of fossil organic carbon during bedrock erosion and export from these headwaters, in common with findings from the French Alpes-de-Haute-Provence (Graz et al., 2011), although oxidation may occur during onward transport and floodplain storage (Bouchez et al., 2010).

The effect of the different rating curve exponents is illustrated by comparing the proportional yields of each component at different discharges, with the largest flows transporting a greater proportion of nfPOC than tPOC, and a greater proportion of tPOC than SS and fPOC. We define three discharge class boundaries, corresponding to Q/Q_{mean} = 1, 10 and 60. Q/Q_{mean} = 10 is the threshold above which POC is added, while Q/Q_{mean} = 60 is the approximate limit of discharges we have sampled. This limit is only exceeded very rarely (5.4×10^{-5} of the time), but can be exceeded substantially: the largest discharge recorded in the 10-minute dataset during the monitoring period was 11950 l s^{-1} (Q/Q_{mean} ~309), on 25 July 1984. Our results show that the lowest discharge class (the state of the stream for over three quarters of the time) is insignificant in terms of both SS and POC export and POC would be dominated by fossil origin (modeled F_{nf} =0.30). Conversely, if the same rating curve applied above the upper limit, discharges of Q/Q_{mean} >60 would transport considerable quantities of sediment, POC and particularly nfPOC (10, 12 and 13% of total transport respectively), despite occurring less than 0.01% of the time. Beyond Q/Q_{mean} = 60, F_{nf} would be 0.76 if the same rating relationship applied. However, because of the lack of constraints on processes or suspended load at these flows, this assumption is not conservative; for example, if landslides are activated, there may be an increase in the proportion of fPOC. Instead, we assume a constant load of all four components for Q/Q_{mean} >60, giving F_{nf} of 0.70 for this discharge range, and conservative estimate for the total yields.

5.3 Sources and Pathways of Non-fossil Organic Carbon in the Erlenbach

In order to draw more general conclusions from the detailed study of nfPOC export in the Erlenbach, the origins and harvesting mechanism of this nfPOC need to be better understood. When there is a small overall load, incidental, local mobilisation dominates and suspended sediment shows the natural variability of catchment composition and process [Figures 2 and 4]. Subsequent POC dilution to a minimum of ~1% [Figure 2] must be due to an increased input of material with low C_{org}, by a mechanism that does not require high-energy flows. This is likely due to higher discharge causing an increase in bed shear stress, which mobilizes fossil-derived material already in the channel. This lithic material (left by previous events, delivered to the channel by creep landslides, or exposed bedrock) contains small amounts of fossil C_{org}: bedrock, bedload, landslide and channel bank pools all have average C_{org} <1%.

Beyond the 500 g s^{-1} threshold (at Q/Q_{mean} ~10), material with a higher C_{org} than bedrock or any of the groups derived from it must be added to the suspended load. Addition of fossil organic carbon released from bedrock, either directly or via landslides and channel banks, cannot explain the compositional trends observed in the suspended load with increasing discharge [Figures 3 and 4]. Instead, the sourcing mechanism must mobilize only surface soil, litter and vegetation, in a way that gives the composition of the non-fossil end member calculated above. This strongly suggests that surface runoff processes are responsible, but there is a compositional discrepancy in $\delta^{15}N$ between runoff suspended sediment and the hypothetical end member. However, the subplots (where the runoff suspended sediment samples were collected) are situated towards the edge of the catchment, whereas runoff entering the stream comes from lower, steeper hillslopes. Here, the bed stress is higher and runoff may penetrate deeper via transient gullying (Horton, 1945), allowing overland flow to pick up more soil and reducing $\delta^{15}N$ values to the hypothetical composition. Considering these processes, hillslope activation driven by surface runoff can account for the change in composition of river suspended sediment POC above background flow, and so for the material added in this hydrological phase. This is supported by end member mixing analysis using dissolved nutrient tracers in the Erlenbach catchment which suggests that, at moderate summer storm peak discharges, over half the runoff in the stream comes directly from precipitation (Hagedorn et al., 2000). The Q/Q_{mean} = 10 threshold, therefore, appears to reflect a critical shear stress at which slope material is mobilised.

The flood hydrographs [Figure 1] suggest that as soon as discharge has peaked, hillslopes are deactivated and delivery of non-fossil organic carbon to the stream is staunched, shown by decrease in C/N and $\delta^{13}C$. This reflects the differing compositions of suspended sediment collected during the rising limb of the hydrograph, when it is usually raining, and falling limb, when it is largely dry. Similarly, the F_{nf} value is significantly higher for samples collected during rainfall (0.54 ± 0.05; $\pm 2\sigma_{mean}$, n = 85) and the rising limb (0.51 ± 0.05; n = 72) than dry periods (0.25 ± 0.06; n = 37) or the falling limb (0.36 ± 0.08; n = 50).

5.4 Caveats

So far we have only considered processes operating during moderate to large flows: having only sampled up to Q/Q_{mean} ~60, we have no insight into the geomorphic dynamic at very high flow rates. If extreme precipitation could trigger rapid landslides, then the system may cross a threshold into a more 'active margin-like' mode of behaviour, where mass wasting during storms causes progressive dilution of modern organic carbon (Blair and Aller, 2012; Kao and Liu, 1996; Masiello and Druffel, 2001).

The calculated F_{nf} of POC exported from the catchment is systematically biased by not including bedload, because bedload is closely related to bedrock [Figure 3] and contains dominantly fossil carbon. This is particularly true in small catchments with high sediment load like the Erlenbach, where bedload is relatively more important than in large mountain rivers (Rickenmann et al., 2012). We chose to exclude bedload in order to enable comparison with other sites, since only suspended load data are available at most locations. However, because bedload transport is constrained to some extent in the Erlenbach, we briefly discuss the implications. The total sediment volume accumulated in the retention basin between August 1982 and October 2012 was 17730 m^3, including pore space and suspendable fines. Using a bulk density of 1750 kg m^{-3} (Rickenmann and McArdell, 2007), and assuming that 75-80% of the material is larger than 2 mm, this gives ~800 tonnes per year. Using the bedrock C_{org} of 0.54%, this equates to an additional ~4 tonnes of organic carbon per year. An alternative estimate, assuming that bedload volume is approximately equal to suspended load volume in the Erlenbach (Turowski et al., 2010), gives an additional ~7 tonnes of organic carbon per year. These figures suggest that, if bedload as well as suspended load is considered, the overall F_{nf} would decrease from 0.6 [Table 5] to between 0.4 and 0.5. A further consideration is the possibility that non-fossil carbon in the form of coarse woody debris is transported in the bedload, meaning that total nfPOC export is also underestimated by our analysis. However, more work is needed to quantify this.

Additional biases may result from the fact that our rating curves and flux estimates are based on samples collected during the summer only and so take no account of possible seasonal changes in the relationships between discharge and tPOC, fPOC and nfPOC concentrations. It is likely that significantly different processes to those we have constrained occur only during the winter and early spring, when there is snow on the ground or melting. The last panel in Figure 1 shows that, although discharge is highest during snow melt in April-May, suspended sediment concentrations are relatively low throughout winter and spring. Multiplying mean discharge by mean

SSC gives mean total suspended load values of ~3 g s^{-1} for winter/spring (December-May) and ~15 g s^{-1} for summer/autumn (June-November). Thus, the mass of material exported under the conditions we have constrained is approximately five times greater than that exported at other times. Even if somewhat different processes were shown to operate in winter and taken into account, the long-term fluxes would not change substantially and our conclusions would be unaffected.

5.5 Global Significance of POC Flux and Processes Observed in the Erlenbach

The rate of export of non-fossil POC from the Erlenbach (14.0 ± 4.4 tonnes km^{-2} yr^{-1}) is broadly comparable to yields of non-fossil POC reported from Taiwan (21 ± 10 tonnes km^{-2} yr^{-1}) (Hilton et al., 2012a) and New Zealand (~39 tonnes km^{-2} yr^{-1}) (Hilton et al., 2008a), and an order of magnitude greater than from the Ganges-Brahmaputra basin (~3 tonnes km^{-2} yr^{-1}) (Galy et al., 2007b). However, the real significance lies in the contrasting processes responsible for these fluxes and their geographical scope. In some mountainous settings, high rates of tectonic uplift, often combined with intense cyclonic storms, drive deep-seated landsliding and flooding on a scale and frequency not seen elsewhere. In contrast, runoff-driven hillslope activation observed in the Erlenbach are widely applicable and do not require catastrophic events to initiate significant carbon POC export. Similar processes are likely to occur wherever there is rain on steep, soil-mantled hillslopes that are effectively coupled to stream channels so that there is a direct, unfiltered transfer of material into them.

Meybeck (1993) estimated that 18% of total atmospheric (i.e. modern) carbon (overall flux of 542 x 10^{12} g yr^{-1}) is exported as soil-derived POC, or ~98 x 10^{12} g yr^{-1}. A direct comparison with the Erlenbach non-fossil POC flux of 14 tonnes km^{-2} yr^{-1} suggests that ~4.6% of the world's total land area behaving like the Erlenbach could account for this flux. The global area covered by temperate broadleaf and mixed forests is ~13.5 million km^2 (Mace et al., 2005), or 9% of the world's land; if other biomes with the potential to host runoff-driven POC export are included (such as temperate coniferous forests and montane grasslands), this rises to 15%. However, it should be noted that steep topography is also an essential ingredient in creating Erlenbach-like conditions. While the biome classification, based on WWF terrestrial ecoregions (Olson et al., 2001), takes account of some factors related to topography, such as climate, it is unlikely to accurately map the topographic limits for the runoff processes described above. Nevertheless, these considerations tentatively suggest that the contribution to global riverine POC flux, particularly the export of non-fossil POC, from Erlenbach-like settings may be more significant than suggested by extant global estimates.

6. Conclusions

We have characterised the processes responsible for transferring organic carbon from hillslope to stream in an alpine headwater catchment with C_{org}-rich bedrock, a high degree of hillslope-channel coupling and no extreme mass wasting over the timescale of the study. Additionally, we have determined the long-term yields of suspended sediment, total POC, fossil POC and non-fossil POC from this system under moderate conditions.

Suspended sediment exported from the Erlenbach has a mean C_{org} of 1.45 ± 0.06 %. Both concentration and composition of this organic carbon vary systematically with hydrological conditions, although variations over any single hydrograph are highly individual. At low discharge, POC concentration and composition is highly variable, due to natural heterogeneity in the small amount of material transported. As discharge increases (along with total suspended load), in-channel clearing causes initial dilution of POC. At a moderate, frequently-crossed threshold (Q/Q_{mean} = 10), the hillslope becomes active and runoff delivers additional POC to the stream in the form of largely soil-derived biomass, causing a bulk shift to higher C/N and lower $\delta^{13}C$ and $\delta^{15}N$. This is associated with an increase in the F_{nf} from 0.30 during background flow to 0.70 at the highest discharges we have sampled (Q/Q_{mean} ~60). Active precipitation is crucial to the mechanism, with riverine suspended sediment showing greater non-fossil influence and significantly higher F_{nf} during rain and on the rising limb than when the rain has stopped and flow is waning. Landslides and channel bank collapse do not regularly contribute to the POC exported under these conditions, but may be activated at extremely high flow rates.

Rating curves show power law relationships between discharge and four components: suspended sediment, total POC, fossil POC and non-fossil POC. All exponents are >1, with fossil POC the lowest at 1.08. Total POC has a significantly higher exponent than suspended sediment, and non-fossil POC has one greater still. Over the past 29 years, the conservative estimates of average export fluxes of suspended sediment, total POC, fossil POC and non-fossil POC (in tonnes km^{-2} yr^{-1}) were 1648 ± 313, 23.3 ± 5.8, 10.1 ± 1.6 and 14.0 ± 4.4 respectively.

We propose that the runoff-driven export of soil-derived POC observed in the Erlenbach is a model for other temperate forested uplands where there is good connectivity between the hillslope and channel. The yield of non-fossil POC from such settings is of the same order of magnitude as those reported from active margin mountain belts, yet the potential area available for this non-catastrophic mode of POC mobilisation extends to large parts of the Earth's continents. Considering our results in the context of previous global estimates of riverine POC discharge, it seems likely that the collective contribution of settings where these processes operate may be more important than previously thought. If the non-fossil POC exported from the Erlenbach and similar catchments is ultimately buried in the ocean, this mechanism could significantly contribute to carbon dioxide drawdown on geological timescales.

Acknowledgements

This work was completed as part of a PhD studentship funded by NERC, partly via the British Geological Survey's British Universities Funding Initiative (BUFI). Radiocarbon analysis was supported by NRCF grant number 1573.0911. We thank staff at WSL, the Godwin Institute and the Department of Geography, University of Cambridge, for assistance with field- and lab-work. Two anonymous reviewers gave insightful comments that helped to improve the manuscript, and Mike Ellis provided useful feedback on an earlier version.

References

Andrews, E. D. (1980). Effective and bankfull discharges of streams in the Yampa River basin, Colorado and Wyoming. *J Hydrol* **46**, 311-330, doi:10.1016/0022-1694(80)90084-0

Berner, R. A. (1982). Burial of organic carbon and pyrite sulfur in the modern ocean; its geochemical and environmental significance. *Am J Sci* **282**, 451-473, doi:10.2475/ajs.282.4.451

Blair, N. E., and R. C. Aller (2012). The fate of terrestrial organic carbon in the marine environment. *Annu Rev Mar Sci* **4**, 401-423, doi:10.1146/annurev-marine-120709-142717

Blair, N. E., E. L. Leithold, S. T. Ford, K. A. Peeler, J. C. Holmes, and D. W. Perkey (2003). The persistence of memory: The fate of ancient sedimentary organic carbon in a modern sedimentary system. *Geochim Cosmochim Acta* **67**, 63-73, doi:10.1016/S0016-7037(02)01043-8

Bouchez, J., O. Beyssac, V. Galy, J. Gaillardet, C. France-Lanord, L. Maurice, and P. Moreira-Turcq (2010). Oxidation of petrogenic organic carbon in the Amazon floodplain as a source of atmospheric CO_2. *Geology* **38**, 255-258, doi:10.1130/G30608.1

Brodie, C. R., J. S. L. Casford, J. M. Lloyd, M. J. Leng, T. H. E. Heaton, C. P. Kendrick, and Z. Yongqiang (2011). Evidence for bias in C/N, $\delta^{13}C$ and $\delta^{15}N$ values of bulk organic matter, and on environmental interpretation, from a lake sedimentary sequence by pre-analysis acid treatment methods. *Quat Sci Rev* **30**, 3076-3087, doi:10.1016/j.quascirev.2011.07.003

Carey, A. E., C. B. Gardner, S. T. Goldsmith, W. B. Lyons, and D. M. Hicks (2005). Organic carbon yields from small, mountainous rivers, New Zealand. *Geophys Res Lett* **31**, L15404, doi:10.1029/2005GL023159

Dijkstra, P., A. Ishizu, R. Doucett, S. C. Hart, E. Schwartz, O. V. Menyailo, and B. A. Hungate (2008). 13C and 15N natural abundance of the soil microbial biomass. *Soil Biol Biochem* **38**, 3257-3266, doi:10.1016/j.soilbio.2006.04.005

France-Lanord, C., and L. A. Derry (1994). $\delta^{13}C$ of organic carbon in the Bengal Fan: Source evolution and transport of C3 and C4 plant carbon to marine sediments. *Geochim Cosmochim Acta* **58**, 4809-4814, doi:10.1016/0016-7037(94)90210-0

France-Lanord, C. and L. A. Derry (1997). Organic carbon burial forcing of the carbon cycle from Himalayan erosion. *Nature* **390**, 65-67, doi:10.1038/36324

Galy, V., J. Bouchez, and C. France-Lanord (2007a). Determination of total organic carbon content and $\delta^{13}C$ in carbonate-rich detrital sediments. *Geostand Geoanal Res* **31**, 199-207, doi:10.1111/j.1751-908X.2007.00864.x

Galy, V., C. France-Lanord, O. Beyssac, P. Faure, H. Kudrass, and F. Palhol (2007b). Efficient organic carbon burial in the Bengal fan sustained by the Himalayan erosional system. *Nature* **450**, 407-410, doi:10.1038/nature06273

Gomez, B., W. T. Baisden, and K. M. Rogers (2010). Variable composition of particle-bound organic carbon in steepland river systems. *J Geophys Res* **115**, F04006, doi:10.1029/2010JF001713

Gordon, E. S., and M. A. Goñi (2003). Sources and distribution of terrigenous organic matter delivered by the Atchafalaya River to sediments in the northern Gulf of Mexico. *Geochim Cosmochim Acta* **67**, 2359-2375, doi:10.1016/S0016-7037(02)01412-6

Graz, Y., C. Di-Giovanni, Y. Copard, M. Elie, P. Faure, F. Laggoun Defarge, J. Lévèque, R. Michels, and J. E. Olivier (2011). Occurrence of fossil organic matter in modern environments: Optical, geochemical and isotopic evidence. *Appl Geochem* **26**, 1302-1314, doi:10.1016/j.apgeochem.2011.05.004

Hagedorn, F., P. Schleppi, P. A. Waldner, and H. Flühler (2000). Export of dissolved organic carbon and nitrogen from Gleysol dominated catchments – The significance of water flow paths. *Biogeochemistry* **50**, 137-161, doi:10.1023/A:1006398105953

Hagedorn, F., J. B. Bucher, and P. Schleppi (2001). Contrasting dynamics of dissolved inorganic and organic nitrogen in soil and surface waters of forested catchments with Gleysols. *Geoderma* **100**, 173-192, doi:10.1016/S0016-7061(00)00085-9

Hatten, J. A., M. A. Goñi, and R. A. Wheatcroft (2012). Chemical characteristics of particulate organic matter from a small, mountainous river system in the Oregon Coast Range. *Biogeochemistry* **107**, 43-66, doi:10.1007/s10533-010-9529-z

Hegg, C., B. W. McArdell, and A. Badoux (2006). One hundred years of mountain hydrology in Switzerland by the WSL. *Hydrol Process* **20**, 371-376, doi:10.1002/hyp.6055

Hilton, R. G., A. Galy, and N. Hovius (2008a). Riverine particulate organic carbon from an active mountain belt: Importance of landslides. *Glob Biogeochem Cycles* **22**, GB1017, doi:10.1029/2006GB002905

Hilton, R. G., A. Galy, N. Hovius, M.-C. Chen, M.-J. Horng, and H. Chen (2008b). Tropical-cyclone-driven erosion of the terrestrial biosphere from mountains. *Nat Geosci* **1**, 759-762, doi:10.1038/ngeo333

Hilton, R. G., A. Galy, N. Hovius, M.-J. Horng, and H. Chen (2010). The isotopic composition of particulate organic carbon in mountain rivers of Taiwan. *Geochim Cosmochim Acta* **74**, 3164-3181, doi:10.1016/j.gca.2010.03.004

Hilton, R. G., A. Galy, N. Hovius, S.-J. Kao, M.-J. Horng, and H. Chen (2012). Climatic and geomorphic controls on the erosion of terrestrial biomass from subtropical mountain forest. *Glob Biogeochem Cycles* **26**, GB3014, doi:10.1029/2012GB004314

Horton, R. E. (1945). Erosional development of streams and their drainage basins; hydrophysical approach to quantitative morphology. *Geol Soc Am Bull* **56**, 275-370, doi:10.1130/0016-7606(1945)56[275:EDOSAT]2.0.CO;2

Kao, S.-J., and K.-K. Liu (1996). Particulate organic carbon export from a subtropical mountainous river (Lanyang Hsi) in Taiwan. *Limnol Oceanogr* **41**, 1749-1757

Komada, T., E. R. M. Druffel, and S. E. Trumbore (2004). Oceanic export of relict carbon by small mountainous rivers. *Geophys Res Lett* **31**, L07504, doi:10.1029/2004GL019512

Komada, T., E. R. M. Druffel, and J. Hwang (2005). Sedimentary rocks as sources of ancient organic carbon to the ocean: An investigation through $\Delta^{14}C$ and $\delta^{13}C$ signatures of organic compound classes. *Glob Biogeochem Cycles* **19**, GB2017, doi:10.1029/2004GB002347

Leithold, E. L., N. E Blair, and D. W. Perkey (2006). Geomorphologic controls on the age of particulate organic carbon from small mountainous and upland rivers. *Glob Biogeochem Cycles* **20**, GB3022, doi:10.1029/2005GB002677

Lyons, W. B., C. A. Nezat, A. E. Carey, and D. M. Hicks (2002). Organic carbon fluxes to the ocean from high-standing islands. *Geology* **30**, 443-446, doi:10.1130/0091-7613(2002)030<0443:OCFTTO>2.0.CO;2

Mace, G., H. Masundire, and J. Baillie (2005). Biodiversity, in *Ecosystems and Human Well-being: Current State and Trends, Volume 1 (Millennium Ecosystem Assessment Report)*, edited by Hassan, R., R. Scholes, and N. Ash, pp. 77-122, Island Press, USA

Masiello, C. A., and E. R. M. Druffel (2001). Carbon isotope geochemistry of the Santa Clara River. *Glob Biogeochem Cycles* **15**, 407-416, doi:10.1029/2000GB001290

Meybeck, M. (1993). Riverine transport of atmospheric carbon: Sources, global typology and budget. *Water Air Soil Poll* **70**, 443-463, doi:10.1007/BF01105015

Milliman, J. D., and J. P. M. Syvitski (1992). Geomorphic/tectonic control of sediment discharge to the ocean: the importance of small mountainous rivers. *J Geol* **100**, 525-544

Nash, D. B. (1994). Effective sediment-transporting discharge from magnitude-frequency analysis. *J Geol* **102**, 79-95

Olson, D. M, E. Dinerstein, E. D. Wikramanayake, N. D. Burgess, G. V. N. Powell, E. C. Underwood, J. A. D'amico, I. Itoua, H. E. Strand, J. C. Morrison, C. J. Loucks,

T. F. Allnutt, T. H. Ricketts, Y. Kura, J. F. Lamoreux, W. W. Wettengel, P. Hedao, and K. R. Kassem (2001). Terrestrial ecoregions of the world: a new map of life on Earth. *BioScience* **51**, 933-938, doi:10.1641/00063568(2001)051[0933:TEOTWA]2.0.CO;2

Prahl, F. G., J. R Ertel, M. A. Goñi, M. A. Sparrow, and B. Eversmeyer (1994). Terrestrial organic carbon contributions to sediments on the Washington margin. *Geochim Cosmochim Acta* **58**, 3035-3048, doi:10.1016/0016-7037(94)90177-5

Rickenmann, D. and B. McArdell (2007). Continuous measurement of sediment transport in the Erlenbach stream using piezoelectric bedload impact sensors. *Earth Surf Proc Land* **32**, 1362-1378, doi:10.1002/esp.1478

Rickenmann, D., J. M. Turowski, B. Fritschi, A. Klaiber, and A. Ludwig (2012). Bedload transport measurements at the Erlenbach stream with geophones and automated basket samplers. *Earth Surf Proc Land* **37**, 1000-1011, doi:10.1002/esp.3225

Schleppi, P., N. Muller, H. Feyen, A. Papritz, J. B. Bucher, and H. Flühler (1998). Nitrogen budgets of two small experimental forested catchments at Alptal, Switzerland. *Forest Ecol Manag* **101**, 177-185, doi:10.1016/S0378-1127(97)00134-5

Schleppi, P., N. Muller, P. J. Edwards, and J. B. Bucher (1999). Three years of increased nitrogen deposition do not affect the vegetation of a montane forest ecosystem. *Phyton* **39**, 197-204

Schleppi, P., Hagedorn, F., and I. Providoli (2004). Nitrate leaching from a mountain forest ecosystem with gleysols subjected to experimentally increased N deposition. *Water, Air and Soil Pollution: Focus* **4**, 453-467, doi:10.1023/B:WAFO.0000028371.72044.fb

Schleppi, P., P. A. Waldner, and B. Fritschi (2006). Accuracy and precision of different sampling strategies and flux integration methods for runoff water: Comparisons based on measurements of the electrical conductivity. *Hydrol Proc* **20**, 395-410, doi:10.1002/hyp.6057

Schuerch, P., A. L. Densmore, B. W. McArdell, and P. Molnar (2006). The influence of landsliding on sediment supply and channel change in a steep mountain catchment. *Geomorphology* **78**, 222-235, doi:10.1016/j.geomorph.2006.01.025

Turowski, J. M, E. M. Yager, A. Badoux, D. Rickenmann, and P. Molnar (2009). The impact of exceptional events on erosion, bedload transport and channel stability in a step-pool channel. *Earth Surf Proc Land* **34**, 1661-1673, doi:10.1002/esp.1855

Turowski, J.M., D. Rickenmann and S.J. Dadson (2010). The partitioning of the total sediment load of a river into suspended load and bedload: a review of empirical data. *Sedimentology* **57**, 1126-1146, doi:10.1111/j.1365-3091.2009.01140.x

Turowski, J. M., A. Badoux, and D. Rickenmann (2011). Start and end of bedload transport in gravel-bed streams. *Geophs Res Lett* **38**, L04401, doi:10.1029/2010GL046558

West, A. J., C.-W. Lin, T.-C. Lin, R. G. Hilton, S.-H. Liu, C.-T. Chang, K.-C. Lin, A. Galy, R. B. Sparkes, and N. Hovius (2011). Mobilization and transport of coarse woody debris to the oceans triggered by an extreme tropical storm. *Limnol Oceanogr* **56**, 77-85, doi:10.4319/lo.2011.56.1.0077

Wheatcroft, R. A., M. A. Goñi, J. A. Hatten, G. B. Pasternack, and J. A. Warrick (2010). The role of effective discharge in the ocean delivery of particulate organic carbon by small, mountainous river systems. *Limnol Oceanogr* **55**, 161-171, doi:10.4319/lo.2010.55.1.0161

Winkler, W., W. Wildi, J. van Stuijvenberg, and C. Caron (1985). Wägital-Flysch et autres flyschs penniques en Suisse Centrale: Stratigraphie, sédimentologie et comparaisons. *Eclogae Geol Helv* **78**, 1-22

Wright, R. F., and L. Rasmussen (1998). Introduction to the NITREX and EXMAN projects. *Forest Ecol Manag* **101**, 1-7, doi:10.1016/S0378-1127(97)00120-5

Figure Captions

Figure 1. Hydrographs for 3 of the 5 storm events sampled in July 2010. Dark grey area is precipitation (x 100, in mm); light grey area is discharge (Q, in $l\ s^{-1}$). Suspended sediment concentration (SSC, x 100, in $g\ l^{-1}$), organic carbon concentration (C_{org}, in %), carbon isotopic composition ($\delta^{13}C$ in ‰), and organic carbon to nitrogen ratio (C/N) are represented by circles, squares, triangles, and diamonds, respectively. Final panel shows the average annual hydrograph over the 29-year monitoring period (1983-2011), and mean suspended sediment concentrations of samples collected every 1-2 weeks over a 6-year period (2005-2010) (SSC data from the Swiss National River Monitoring and Survey Programme, http://www.eawag.ch/forschung/wut/schwerpunkte/chemievonwasserresourcen/naduf/datendownload_EN).

Figure 2. Variation of organic carbon concentration in riverine suspended sediment with total suspended load (note logarithmic *x*-axis). Open symbols are background flow (Q/Q_{mean} <10). POC = particulate organic carbon.

Figure 3. Top: nitrogen to carbon ratios (N/C) and carbon isotopic composition ($\delta^{13}C$) of Erlenbach riverine suspended sediment, hillslope runoff suspended sediment and major stores of carbon within the catchment. Bottom: carbon to nitrogen ratios (C/N) and nitrogen isotopic composition ($\delta^{15}N$) of the same pools.

Figure 4. Zoomed-in views of the plots in Figure 3, where suspended sediment samples are colour-coded according to total suspended load (warm colours represent

low values; cold colours represent high values). Open squares are background flow (Q/Q_{mean} <10). 'Fossil end member' includes bedrock, bedload, channel banks and landslides. Dotted lines indicate potential mixing zones between the fossil end member and non-fossil sources. Determination and nature of the hypothetical non-fossil end member is discussed section 5.1.

Figure 5. Rating curves showing power law relationships between Q/Q_{mean} and suspended sediment concentration, total POC (tPOC), fossil POC (fPOC) and non-fossil POC (nfPOC), all in mg l^{-1}. POC is particulate organic carbon concentration. Small squares represent individual samples; open symbols are background flow (Q/Q_{mean} <10). Dashed lines are 95% confidence bands.

Table 1. Characteristics of the five storm events sampled.

Date	**Approx. time (UTC+2)**	**Number of samples**[a]	**Peak Q ($l\ s^{-1}$)**	**Peak Q/Q_{mean}**[b]
12 July 2010	19.00-20.30	37	2290	59
22-23 July 2010	20.30-02.30	37 + 1 preceding	420	11
26 July 2010	21.00-00.00	16 + 1 preceding	300	8
29 July 2010	06.30-16.45	25	1190	31
30 July 2010	08.45-16.00	9	1580	41

[a]Additional samples for 22 and 26 July were collected at intervening low flow.
[b]Q/Q_{mean} is the discharge relative to the average discharge over the period 1983-2011 inclusive (38.6 $l\ s^{-1}$).

Table 2. Organic carbon concentration (C_{org}), carbon to nitrogen ratio (C/N), carbon isotopic composition ($\delta^{13}C$) and nitrogen isotopic composition ($\delta^{15}N$) of major carbon stores within the catchment, and hillslope runoff and riverine suspended sediment[a].

	n	C_{org} (%)		C/N		$\delta^{13}C$ (‰)		$\delta^{15}N$ (‰)	
		Mean	**σ**	**Mean**	**σ**	**Mean**	**σ**	**Mean**	**σ**
Bedrock	22	0.54 ± 0.11	0.26	7.81 ± 1.7	3.98	-25.71 ± 0.36	0.84	3.34 ± 0.26	0.60
Bedload	11	0.87 ± 0.21	0.36	9.78 ± 0.9	1.57	-25.84 ± 0.10	0.17	2.13 ± 0.23	0.38
Channel banks	8	0.87 ± 0.22	0.32	8.12 ± 1.1	1.58	-25.89 ± 0.40	0.57	2.91 ± 0.29	0.40
Landslide profile	22	0.64 ± 0.06	0.15	7.38 ± 0.4	0.87	-26.03 ± 0.12	0.28	2.67 ± 0.30	0.71
Deep soil[b]	10	2.15 ± 1.2	1.85	11.8 ± 2.3	3.64	-25.98 ± 0.34	0.54	3.56 ± 1.99	3.14
Surface soil[b]	17	16.5 ± 6.3	12.9	17.9 ± 2.2	4.45	-26.84 ± 0.48	0.98	-1.33 ± 0.77	1.59
Foliage	8	46.9 ± 2.0	2.88	55.5 ± 17	24.2	-28.30 ± 1.13	1.60	-5.87 ± 1.67	2.36
Woody debris	12	49.1 ± 1.8	3.18	173 ± 98	170	-25.25 ± 0.69	1.19	-3.99 ± 1.29	2.24
Hypothetical non-fossil end member	-	-	-	*15.8 ± 6.8*	-	*-27.15 ± 0.53*	-	*0.61 ± 1.40*	-
Forest hillslope runoff	38	9.12 ± 0.9	2.77	12.6 ± 0.7	2.28	-26.50 ± 0.08	0.23	2.48 ± 0.30	0.93
Meadow hillslope runoff	10	15.9 ± 1.7	2.67	12.6 ± 1.8	2.91	-26.56 ± 0.50	0.79	4.43 ± 1.04	1.64
Riverine suspended sediment[c]	122	1.45 ± 0.06	0.32	9.55 ± 0.2	1.34	-26.33 ± 0.08	0.45	2.21 ± 0.16	0.87
Rising limb	*72*	*1.36 ± 0.07*	*0.29*	*9.89 ± 0.3*	*1.35*	*-26.45 ± 0.08*	*0.32*	*1.95 ± 0.13*	*0.56*
Falling limb	*50*	*1.57 ± 0.09*	*0.33*	*9.16 ± 0.4*	*1.29*	*-26.16 ± 0.15*	*0.54*	*2.58 ± 0.31*	*1.09*
Raining	*85*	*1.40 ± 0.06*	*0.29*	*10.0 ± 0.3*	*1.32*	*-26.49 ± 0.07*	*0.34*	*1.94 ± 0.12*	*0.53*
Dry	*37*	*1.55 ± 0.12*	*0.37*	*8.69 ± 0.4*	*1.07*	*-25.98 ± 0.15*	*0.47*	*2.83 ± 0.38*	*1.15*

[a]σ = standard deviation; errors are ± twice the standard error on the mean.
[b]Surface soil samples were collected from the top ~10cm (without overlying vegetation); deep soil samples were collected from below 10 cm in two vertical profiles.
[c]Riverine suspended sediment is subdivided into samples collected during i) rising and falling limbs and ii) active rainfall and dry periods.

Table 3. Results of radiocarbon analysis on selected samples[a].

Sample Type	Q (l s^{-1})	Sample ID	Publication code	C_{org} (%)	F_{mod} (fraction of modern C)[b]	$\Delta^{14}C$ (‰)	Conventional radiocarbon age (years BP)
Suspended sediment	78	12.7 1748	SUERC-40494	2.2	0.68 ± 0.004	-317.9 ± 3.5	3073 ± 41
	394	12.7 1719	SUERC-39226	1.2	0.67 ± 0.003	-328.0 ± 3.2	3193 ± 38
	517	29.7 1768	SUERC-39232	1.3	0.47 ± 0.002	-530.5 ± 2.3	6074 ± 39
	1170	12.7 1711	SUERC-39229	2.2	0.74 ± 0.004	-256.5 ± 3.5	2381 ± 38
	2060	12.7 1707	SUERC-39230	1.9	0.69 ± 0.003	-314.4 ± 3.2	3033 ± 38
	2290	12.7 1729	SUERC-39231	1.8	0.67 ± 0.003	-333.8 ± 3.2	3262 ± 38
Surface soil		ER-ST-1-L-0	SUERC-39216	1.2	0.53 ± 0.003	-471.7 ± 2.6	5123 ± 39
		ER-ST-2-L-15	SUERC-39219	6.0	1.00 ± 0.005	-3.5 ± 4.7	Modern
		ER-ST-1-R-350	SUERC-39220	25	1.06 ± 0.005	64.8 ± 5.0	Modern
		ER-ST-1-R-20	SUERC-39221	11	1.05 ± 0.005	53.9 ± 5.0	Modern
Wood entrained in bedload		ER-V-19	SUERC-39222	50	0.81 ± 0.004	-186.5 ± 3.8	1658 ± 37
		ER-V-11	SUERC-39223	50	1.00 ± 0.005	-0.1 ± 4.5	Modern
Wood entrained in landslides		ER-V-17	SUERC-39224	52	0.87 ± 0.004	-132.1 ± 4.1	1138 ± 38
		ER-V-20	SUERC-39225	50	0.61 ± 0.003	-392.9 ± 2.7	4009 ± 36

[a]Errors are ±1σ.
[b]Reference date for F_{mod} is 1950; therefore F_{mod} can be >1 in plants and soils due to incorporation of ^{14}C from nuclear weapons testing during the second half of the twentieth century.

Table 4. Rating curve parameters for power law relationships between Q/Q_{mean} and suspended sediment (SS) or particulate organic carbon (POC), of the form SS or POC = $a(Q/Q_{mean})^{b}$ [(a)].

	a	***b***	**R^{2}[(b)]**	**Q_e ($l\ s^{-1}$)[c]**	**Q_e (Q/Q_{mean})[c]**
SS	99.7 ± 29.4 *96.0 ± 44.2*	1.19 ± 0.08 *1.20 ± 0.12*	0.78 *0.68*	300	7.7
tPOC	0.96 ± 0.30 *0.96 ± 0.48*	1.33 ± 0.08 *1.33 ± 0.13*	0.81 *0.71*	400	10.4
fPOC	0.80 ± 0.39 *0.75 ± 0.64*	1.08 ± 0.13 *1.10 ± 0.23*	0.50 *0.32*	230	5.6
nfPOC	0.41 ± 0.20 *0.44 ± 0.33*	1.45 ± 0.13 *1.43 ± 0.20*	0.70 *0.57*	520	13.4

[a]Values in regular type (used for flux calculations) are based on the whole sample set; values in italics are based only on samples with Q/Q_{mean}>10. There are three classes of POC: total (tPOC), fossil (fPOC) and non-fossil (nfPOC).
[b]Correlation coefficients are given as R^2.
[c]Q_e is the effective discharge, as defined by Wheatcroft et al. (2010). Q/Q_{mean} is the discharge relative to the average discharge over the period 1983-2011 inclusive (38.6 $l\ s^{-1}$).

Table 5. Modeled export of suspended sediment (SS) and total, fossil and non-fossil particulate organic carbon (tPOC, fPOC and nfPOC), averaged over 29 years (1983-2011 inclusive).

	Mean annual yield (tonnes)	**Mean annual yield (tonnes) according to Q/Q_{mean} ($l\ s^{-1}$). Proportions in each class are given in brackets.**				**Export flux (t $km^{-2}\ yr^{-1}$)**
		$Q/Q_{mean} \leq 1$ (77%)	**$1 < Q/Q_{mean} \leq 10$ (22%)**	**$10 < Q/Q_{mean} \leq 60$ (1%)**	**$Q/Q_{mean} > 60$[b] (<0.01%)**	
SS	1220 ± 232	12.0 ± 0.79 (1.1%)	376 ± 35.3 (32%)	740 ± 91.8 (61%)	91.1 ± 61.3 (5.8%) *215 ± 171 (10%)*	1648 ± 313
tPOC	17.3 ± 4.3	0.11 ± 0.01 (0.7%)	4.57 ± 0.44 (28%)	11.0 ± 1.40 (64%)	1.57 ± 1.06 (6.9%) *4.21 ± 3.43 (12%)*	23.3 ± 5.8
fPOC	7.44 ± 1.2	0.10 ± 0.01 (1.5%)	2.56 ± 0.24 (36%)	4.30 ± 0.53 (58%)	0.47 ± 0.32 (5.1%) *1.02 ± 0.79 (8.6%)*	10.1 ± 1.6
nfPOC	10.4 ± 3.2	0.04 ± 0.00 (0.5%)	2.39 ± 0.23 (26%)	6.85 ± 0.88 (67%)	1.10 ± 0.74 (7.3%) *3.29 ± 2.73 (13%)*	14.0 ± 4.4
F_{nf}[a]	0.61 ± 0.02	0.30 ± 0.00	0.48 ± 0.00	0.61 ± 0.00	0.70 ± 0.00 *0.76 ± 0.02*	-

[a]F_{nf} is the modeled fraction of organic carbon derived from non-fossil sources, given overall in the first column and then for separate discharge classes.
[b]For Q/Q_{mean} >60, the top line (normal type; used in calculating overall yields and fluxes) assumes that the rating curves are flat from Q/Q_{mean} = 60; the bottom line (italics; given for comparison only) assumes that the same rating relationships apply above this limit.

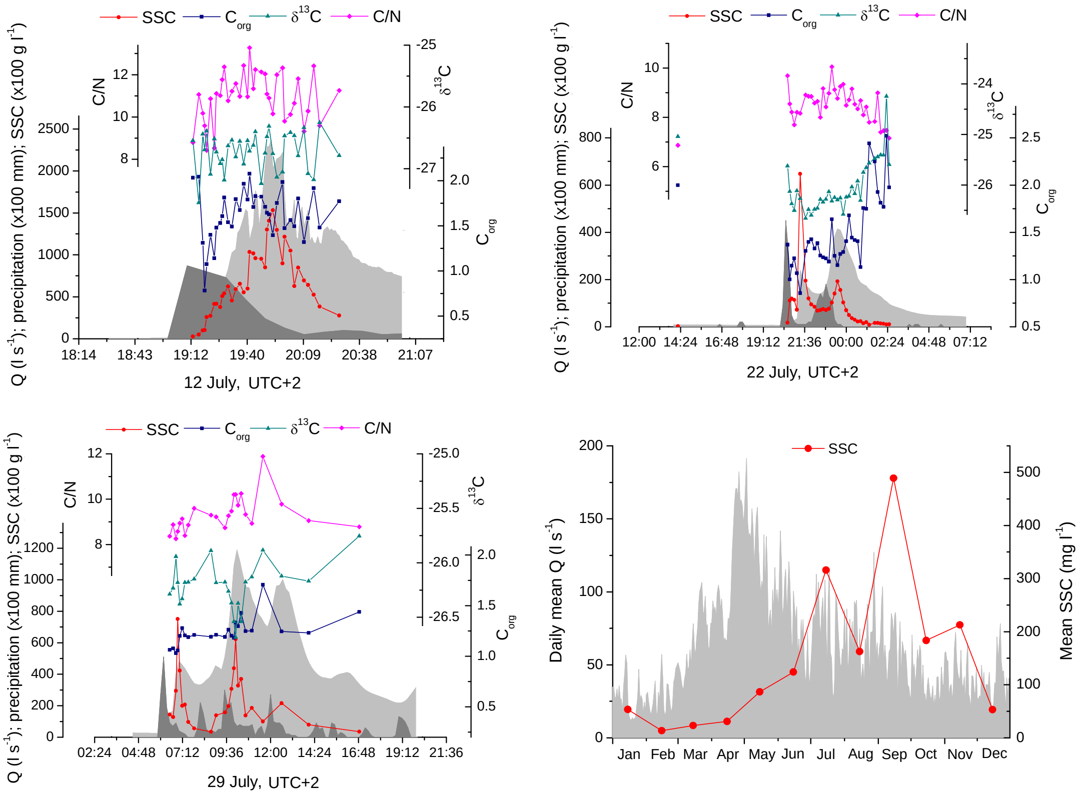

Figure 1

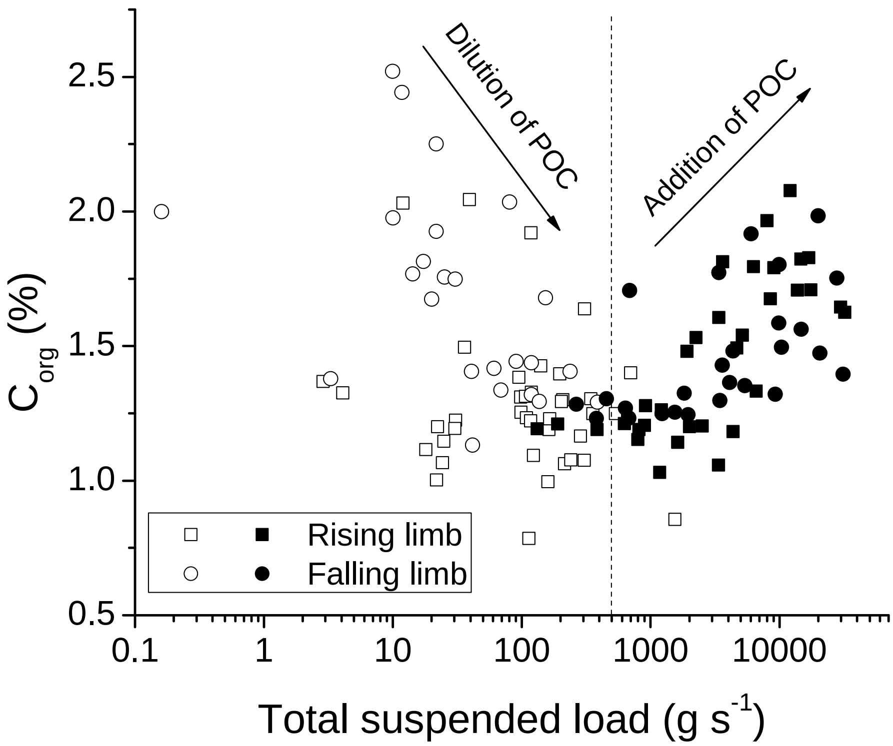

Figure 2

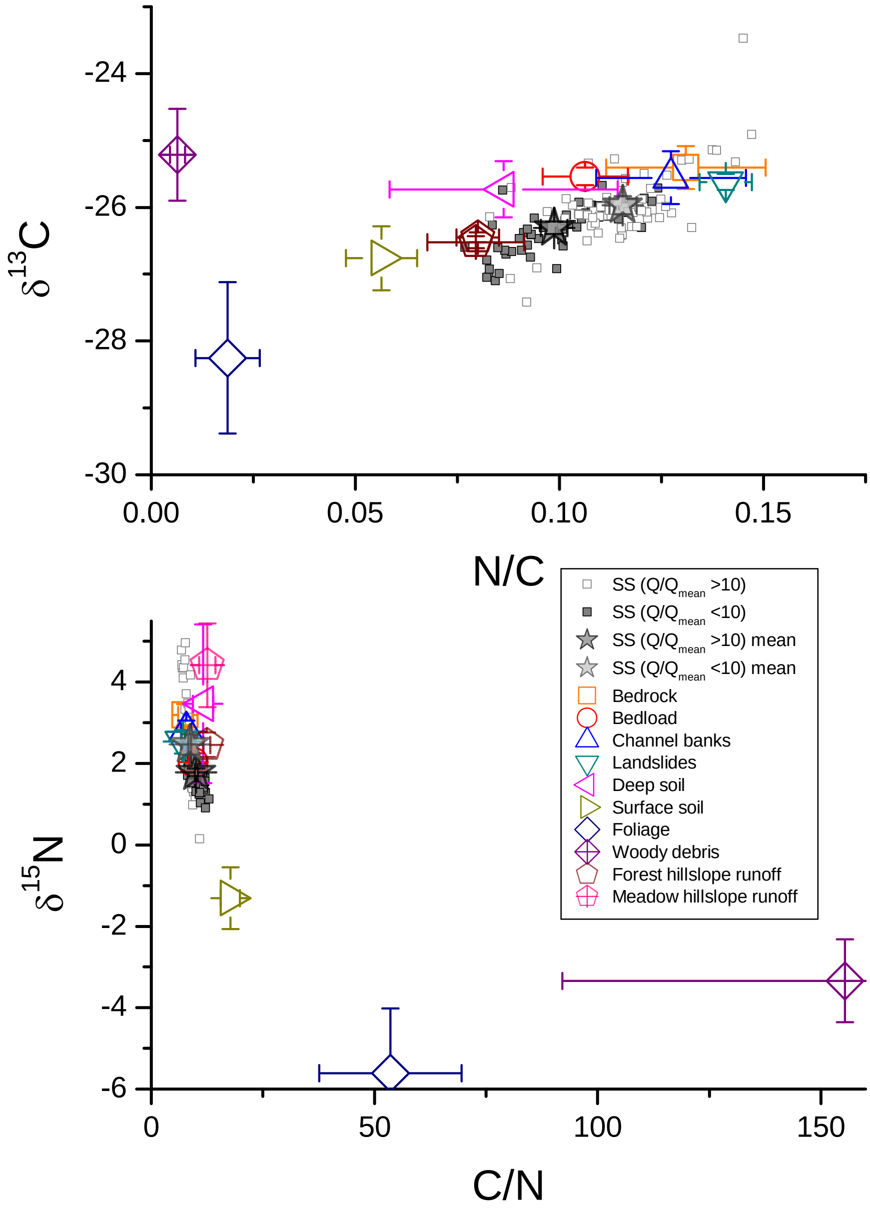

-24
-26
-28
-30
0.00
0.05
0.10
0.15
N/C
δ13C
SS (Q/Qmean >10)
SS (Q/Qmean <10)
SS (Q/Qmean >10) mean
SS (Q/Qmean <10) mean
Bedrock
Bedload
Channel banks
Landslides
Deep soil
Surface soil
Foliage
Woody debris
Forest hillslope runoff
Meadow hillslope runoff
4
2
0
-2
-4
-6
0
50
100
150
C/N
δ15N

Figure 3

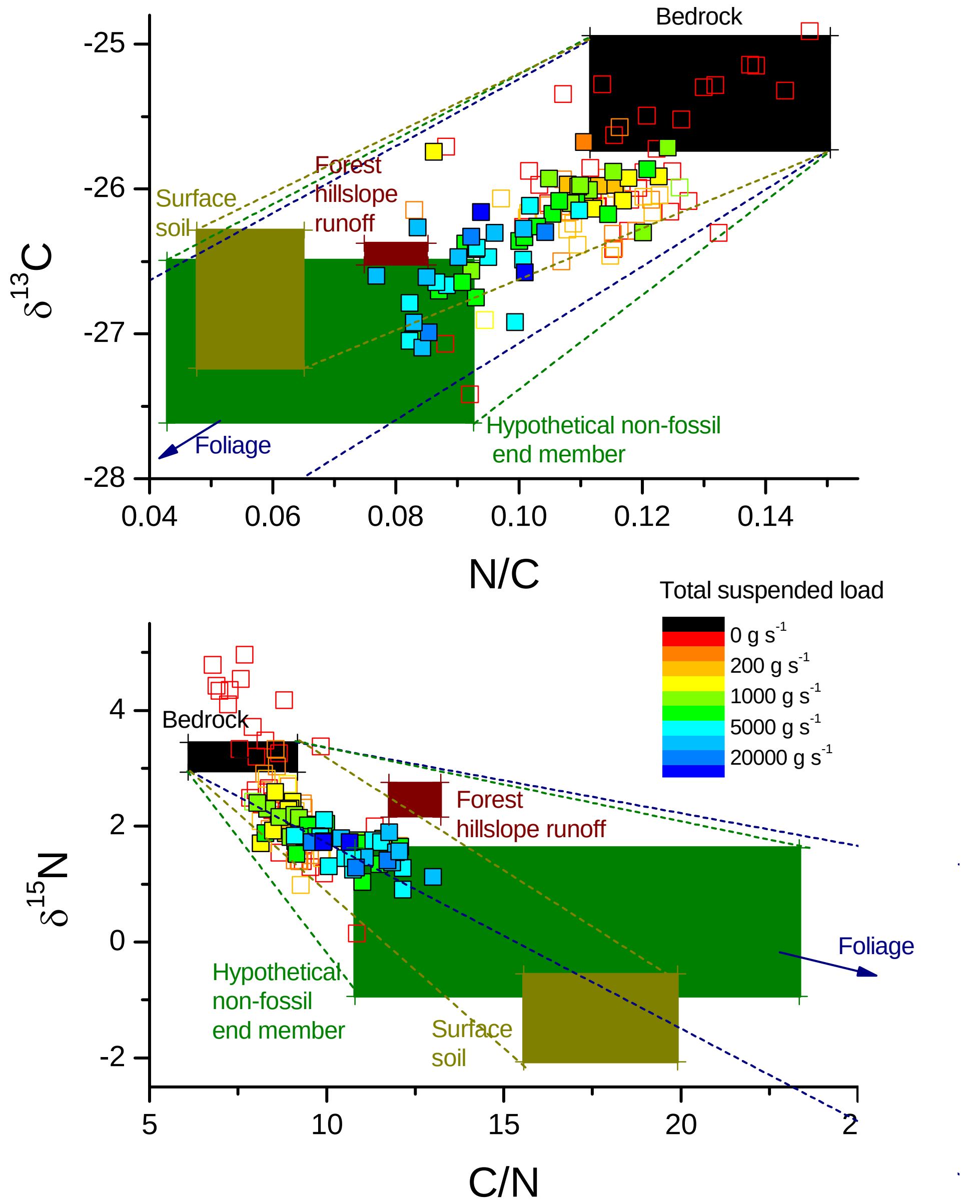

Bedrock
-25
-26
-27
-28
Forest
hillslope
runoff
Surface
soil
Foliage
Hypothetical non-fossil
end member
δ13C
0.04
0.06
0.08
0.10
0.12
0.14
N/C
Total suspended load
0 g s-1
200 g s-1
1000 g s-1
5000 g s-1
20000 g s-1
4
2
0
-2
Bedrock
Forest
hillslope runoff
Foliage
Hypothetical
non-fossil
end member
Surface
soil
δ15N
5
10
15
20
2
C/N

Figure 4

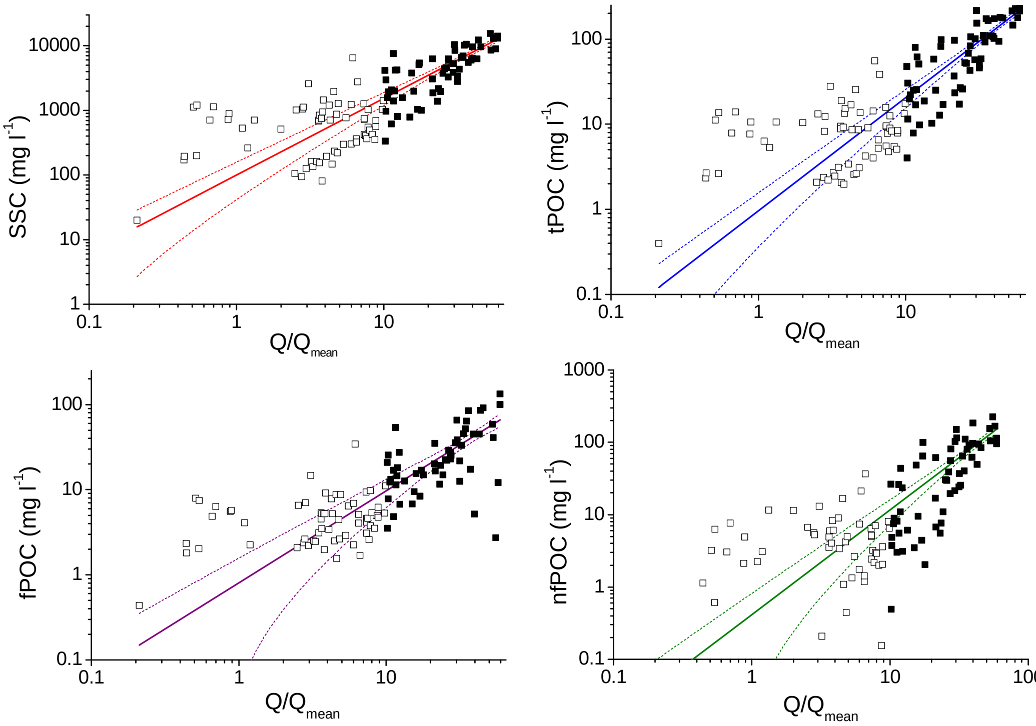
SSC (mg l-1)
tPOC (mg l-1)
fPOC (mg l-1)
nfPOC (mg l-1)
Q/Qmean
Q/Qmean
Q/Qmean
Q/Qmean
1
10
100
1000
10000
0.1
1
10
100
1000

Figure 5